Electrical and thermoelectrical properties of SnTe-based films and superlattices

Akihiro Ishida,[1,a)] Tomohiro Yamada,[1] Takuro Tsuchiya,[1] Yoku Inoue,[1] Sadao Takaoka,[2] and Takuji Kita[3]
[1]*Department of Electrical and Electronic Engineering, Shizuoka University, Johoku 3-5-1, Naka-ku, Hamamatsu 432-8561, Japan*
[2]*Department of Physics, Graduate School of Science, Osaka University, Machikaneyama 1-1, Toyonaka 560-0043, Japan*
[3]*Toyota Motor Co., Mishuku 1200, Susono 410-1193, Japan*

(Received 8 June 2009; accepted 30 August 2009; published online 23 September 2009)

SnTe-based films and superlattices (SLs) were prepared and their electrical properties were measured. A EuTe/SnTe SL exhibited a hole mobility of 2720 $cm^2/V\,s$, which is the highest value reported for any semiconductor material at room temperature. The SnEuTe film also exhibited high hole mobility in contrast to the PbEuTe system. These properties are explained in terms of the band offsets of EuTe/SnTe heterojunction and a decrease in the number of Sn vacancies. In addition, SnTe/PbSe and SnTe/PbS SLs with thin SnTe layers displayed *n*-type conduction with Seebeck coefficients comparable to those for PbSe and PbS. These properties reflect the type II heterostructures. © *2009 American Institute of Physics*. [doi:10.1063/1.3236541]

IV-VI compound semiconductors and quantum wells have a wide range of applications such as thermoelectric devices, infrared lasers, and detectors. Among these IV-VI materials, lead chalcogenides have been most extensively studied. On the other hand, SnTe-based materials have not received the attention owing to the high carrier concentration of SnTe. Although SnTe has a very small Seebeck coefficient, certain applications can be envisaged using quantum well systems which utilize the special band offsets with other materials such as SnTe/PbTe system. We previously proposed that the SnTe/PbTe heterojunction becomes type II where the valence band maxima of SnTe situate above the conduction band minima of PbTe,[1] and explained the semimetallic properties of SnTe/PbTe superlattices (SLs) in this manner.[2,3] Rogacheva *et al.*[4] reported the electrical and Seebeck properties of SnTe/PbTe SLs, and attempted to explain their nonmonotonic dependence on the SnTe layer thickness by the coexistence of electrons and holes. These properties can be explained by the type II band offsets of the heterojunction. In this study, the electrical properties of EuTe/SnTe, SnTe/PbSe, and SnTe/PbS SLs and SnEuTe films, including their Seebeck properties, are investigated and are discussed in terms of the band offsets at the heterojunctions.

Figure 1 shows the band diagram of a SnTe/PbTe SL proposed by Murase *et al.*,[1] including schematic subband structures and corresponding optical transitions. Real subband structures are more complicated owing to anisotropic effective masses of *L*-point valleys for PbTe and SnTe. Solid lines show conduction band subbands in the PbTe well, and dashed lines show valence band subbands in the SnTe well. In the SnTe/PbSe and SnTe/PbS SLs, similar band diagrams are expected. In the SnTe/PbTe type II heterostructure, the valence band electrons in SnTe flow into the conduction band of PbTe. Thus, the SL becomes semimetallic, as ascertained by Hall measurements of SnTe/PbTe SLs.[2,3] If the thickness of SnTe in the SnTe/PbTe SL is decreased, the number of electrons flowing into the PbTe layer decreases, and the Fermi level approaches the bottom of the PbTe conduction band. Thus, *n*-type conduction similar to that in *n*-type PbTe should appear even if both the PbTe and the SnTe had *p*-type conduction. This phenomenon was reported by Rogacheva *et al.*[4] for *n*-PbTe/*p*-SnTe SLs, and similar behavior should be expected for SnTe/PbSe and SnTe/PbS systems if similar type II heterostructures are formed. Figure 2 shows the band offsets expected for EuTe/PbTe and EuTe/SnTe SLs. EuTe is a wide gap material with a band gap energy approximately 2 eV, and the EuTe/PbTe SL becomes type I, where the PbTe layers form quantum wells for both electrons and holes with comparable barrier heights.[5,6] Considering the band offset of the SnTe/PbTe system, it is expected that the barrier height in the conduction band would be much smaller in the EuTe/SnTe quantum well system, as shown in Fig. 2(b). In this study, the SnTe/PbSe, SnTe/PbS, and EuTe/SnTe, SLs were prepared by hot wall epitaxy.[7] To prepare SnTe/PbSe and SnTe/PbS SLs, 5 N stoichiometric SnTe, PbSe, and PbS polycrystals were used as the source materials. Carrier types of the films prepared from the materials were *p*-type for SnTe and PbSe, and *n*-type for PbS. Carrier concentrations of PbS and PbSe were $\sim 10^{17}$ cm^{-3}

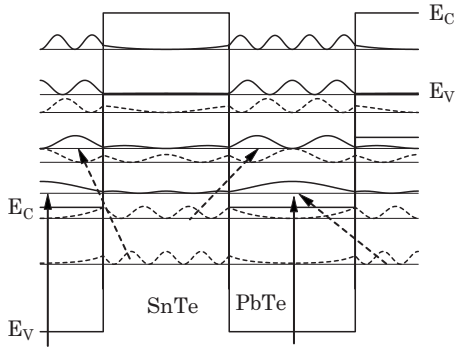

FIG. 1. Schematic band diagram of the SnTe/PbTe SL, subband structures, and possible optical transitions.

[a)]Electronic mail: tdaishi@ipc.shizuoka.ac.jp. Tel.: +81-53-478-1104.

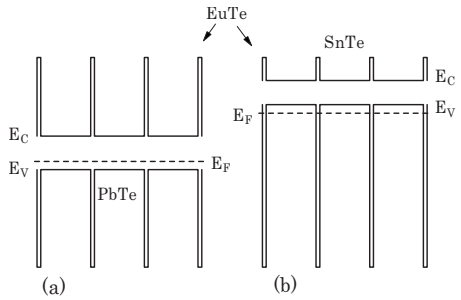

FIG. 2. Schematic energy band diagrams for EuTe/PbTe and EuTe/SnTe SLs.

and those of SnTe were 2×10^{20} cm^{-3}. To prepare the EuTe/SnTe SL, 7–26 nm of SnTe and one atomic layer of Eu were deposited alternately to compensate for the strong stoichiometric deviation of the SnTe film. $Sn_{1-x}Eu_xTe$ films with $x\approx0.02$ were also prepared by simultaneous deposition of SnTe and Eu. Table I shows the electrical properties of these films and SLs at room temperature. Electrical properties of other IV-VI films and SLs are also shown for comparison.

The SnTe/PbSe SL with thin SnTe layer exhibited *n*-type conduction, even though both of SnTe and PbSe had *p*-type conduction, as expected from the type II band structure. The optical properties of this SL would be expected to be quite different to those of a semiconductor film. Figure 3 shows a comparison of the optical transmission spectra between the PbSe film and SnTe/PbSe SL. Absorption coefficients, determined by simulations assuming an interband absorption and an exponential tail are shown as dashed-dotted lines, and the simulated spectra are shown by dashed line.[6] The SnTe/PbSe SL exhibited strong absorption above the band gap of PbSe (2200 cm^{-1}). The exponential tail observed over the entire spectral range below the band gap of PbSe corresponds to electron transitions from the SnTe valence band to the PbSe conduction band as indicated by the dashed arrows in Fig. 1.

TABLE I. Electrical properties of SnTe/PbSe, SnTe/PbS, and EuTe/SnTe SLs and SnEuTe films at room temperature. Electrical properties of other IV-VI films and SLs are also shown for comparison.

Sample	Structure (nm/nm)	μ (cm^2/Vs)	Carrier con. (cm^{-3})	Dopant	S ($\mu V/K$)
SnTe		203	$p=2.0\times10^{20}$	···	6
PbSe		534	$p=3.5\times10^{17}$	···	
PbS		491	$n=7.8\times10^{17}$	···	
PbTe		795	$p=2.3\times10^{18}$	Tl	
PbTe		1410	$n=1.6\times10^{18}$	Bi	
SnTe/PbSe	20/20	107	$p=1.9\times10^{19}$	···	43
SnTe/PbSe	10/20	249	$n=5.1\times10^{18}$	···	−103
SnTe/PbSe	1.5/20	783	$n=1.5\times10^{18}$	···	−254
SnTe/PbS	1.5/25	386	$n=2.8\times10^{18}$	···	−252
SnTe/PbS	2/20	283	$n=2.3\times10^{18}$	···	−266
SnTe/PbS	2.5/30	309	$n=3.8\times10^{18}$	···	−251
$Pb_{0.95}Eu_{0.05}Te$		49.7	$p=1.1\times10^{18}$	Tl	
SnEuTe		1740	$p=1.8\times10^{19}$	···	27
SnEuTe		2110	$p=8.9\times10^{18}$	···	77
EuTe/PbTe	0.3/10	434	$p=2.1\times10^{18}$	Tl	
EuTe/SnTe	0.2/7	1670	$p=1.2\times10^{19}$	···	66
EuTe/SnTe	0.3/14	2080	$p=1.1\times10^{19}$	···	63
EuTe/SnTe	0.4/26	2720	$p=1.0\times10^{19}$	···	68

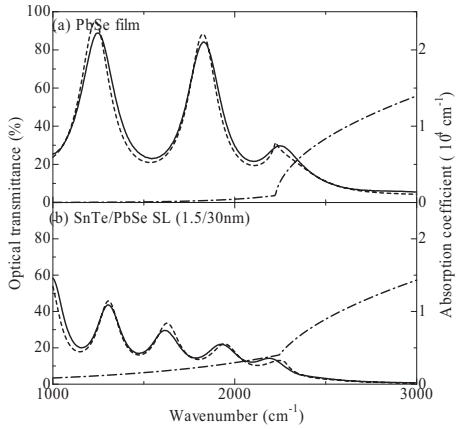

FIG. 3. Optical transmission properties of PbSe film and SnTe/PbSe SL with thickness of 1.6 and 3.1 μm, respectively. Solid and dashed lines show experimental and simulated transmission spectra, and dashed-dotted lines show corresponding absorption coefficients.

In the EuTe/SnTe SL, the hole concentration was greatly reduced compared to the value for SnTe, and the room temperature hole mobility was drastically enhanced, as shown in Table I. A large enhancement in hole mobility was also observed for the SnEuTe ternary alloy films. Usually, the carrier concentration of SnTe decreases with increasing Sn content to 4×10^{19} cm^{-3} with a hole mobility of about 900 $cm^2/V\,s$ owing to the decrease in Sn vacancies.[8,9] There are some reports on the SnEuTe ternally alloy and EuTe/SnTe SL.[10–12] However, reduction in the carrier concentration has never been reported for this system. Thus, it is considered that the insertion of Eu strongly reduced the number of Sn vacancies in the SnTe layer, leading to the reduction in hole concentration and a drastic increase in hole mobility. Normally, in ternary compounds combined with wide gap materials and IV-VI materials (such as PbEuTe in Table I), the electron mobility is much lower than that of the host IV-VI semiconductor films, because the wide gap elements act as strong scattering centers in the films. This effect also occurs in EuTe/PbTe SLs through the interdiffusion of Eu or interface roughness, and the carrier mobility decreases in the SLs. In the EuTe/SnTe SL, the Eu atoms did not act as significant scattering centers, as indicated by the high hole mobility of the SnEuTe film shown in Table I and the decrease in hole concentration resulting from the decrease in Sn vacancies increased the hole mobility dramatically. As shown in Fig. 2(a), the EuTe layer acts as a very high potential barrier for both electrons and holes in the EuTe/PbTe SL, and the random Eu distribution due to interdiffusion of the constituents results in a strong scattering of the carriers. On the other hand, it is considered that the conduction band bottom in EuTe is located near the narrow band gap of SnTe in the EuTe/SnTe SL. In the case of Fig. 2(b), the Fermi level of SnTe even in the *p*-type sample is situated closer to the conduction band bottom of EuTe in the EuTe/SnTe system, as compared with that of PbTe in the EuTe/PbTe system. Thus, the tunneling probability for holes is higher in the EuTe/SnTe system because they experience a potential barrier up to the conduction band bottom of EuTe, and the Eu atoms do not act as strong scattering centers. There is another possibility that the EuTe/SnTe heterojunction becomes type II where the conduction band bottom of EuTe locates below the valence band top of SnTe. Anyway, the conduction band bottom of

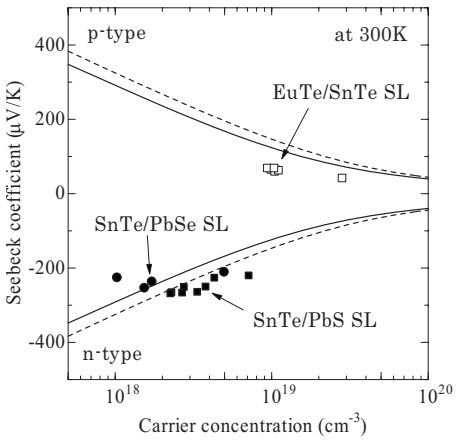

FIG. 4. Seebeck coefficient of SnTe/PbSe, SnTe/PbS, and EuTe/SnTe SLs. Theoretical curves for PbSe and PbS films are indicated as solid and dashed lines, respectively.

EuTe must locate near the valence band top of SnTe to result the SnEuTe in high hole mobility. It is also considered that the large number of Sn vacancies in the SnTe film forms an impurity band in the valence band, which strongly affects the electrical properties. Thus, the strong decreases in the vacancy concentrations in the SnEuTe film and EuTe/SnTe SL demonstrated the high mobility nature of *p*-type SnTe. Room temperature carrier mobilities of polar semiconductors are strongly affected by optical phonon scattering, with Ge having highest hole mobility of 1900 $cm^2/V\,s$ among semiconductor materials owing to the lack of ionicity.[13] However, the EuTe/SnTe SL prepared by alternating 26 nm SnTe and one monolayer of Eu exhibited a hole mobility of 2720 $cm^2/V\,s$ at room temperature, which is the highest value reported for any *p*-type semiconductor.

Figure 4 shows the dependence of the Seebeck coefficient on the carrier concentration for the SnTe/PbSe, SnTe/PbS, and EuTe/SnTe SLs. SnTe layer thickness for the SnTe/PbSe and SnTe/PbS SLs are 20–30 nm, and the thicknesses of the PbSe and PbS layers are less than 2.5 and 5 nm, respectively, where a clear *n*-type conduction appears. The Seebeck coefficient of the EuTe/SnTe SL was independent of the SnTe thickness. Negative and positive values of the Seebeck coefficients correspond to *n*-type and *p*-type conductions, respectively. Theoretical curves for PbSe and PbS films are also drawn as solid and dashed lines, respectively.[14] The Seebeck coefficients of the SnTe/PbSe and SnTe/PbS SLs were comparable with the theoretical values for PbSe and PbS films. The Seebeck coefficient in the EuTe/SnTe system was smaller than the theoretical values for PbSe and PbS. We did not calculate the theoretical values for SnTe and EuTe/SnTe SLs because of the lack of available effective mass data and the complicated band structure around the *L*-points.[15] It is considered that the small Seebeck coefficient is the result of the complicated band structure at the valence band top, where valence band holes at the *L*-point have a negative effective mass.

In conclusion, SnTe/PbSe, SnTe/PbS, and EuTe/PbTe SLs and SnEuTe films were prepared, and their electrical properties were measured at room temperature. The EuTe/SnTe SL showed very high room temperature hole mobility of up to 2720 $cm^2/V\,s$, which is the highest value among semiconductor materials. The high hole mobility was explained by the reduction in the number of Sn vacancies and the small band offset between conduction band bottom of EuTe and valence band top of SnTe. The SnTe/PbSe and SnTe/PbS SLs had a similar band offset to the SnTe/PbTe type II SL, and the SLs with thin SnTe layers showed *n*-type conduction. Optical transmission properties of the SnTe/PbSe SL indicated semimetallic behavior. The Seebeck coefficients of SnTe/PbSe, SnTe/PbS, and EuTe/SnTe SLs were also measured, and the values for the SnTe/PbSe and SnTe/PbS SLs were found to be comparable to the theoretical values for PbSe and PbS films, respectively.

[1] K. Murase, S. Shimomura, S. Takaoka, A. Ishida, and H. Fujiyasu, Superlattices Microstruct. **1**, 177 (1985).
[2] A. Ishida, M. Aoki, and H. Fujiyasu, J. Appl. Phys. **58**, 1901 (1985).
[3] S. Takaoka, T. Okumura, K. Murae, A. Ishida, and H. Fujiyasu, Solid State Commun. **58**, 637 (1986).
[4] I. Rogacheva, O. N. Nashchekina, A. V. Meriuts, S. G. Lyubchenko, M. S. Dresselhaus, and G. Dresselhaus, Appl. Phys. Lett. **86**, 063103 (2005).
[5] A. Ishida, S. Matsuura, M. Mizuno, and H. Fujiyasu, Appl. Phys. Lett. **51**, 478 (1987).
[6] A. Ishida, M. Veis, and Y. Inoue, Jpn. J. Appl. Phys., Part 2 **46**, L281 (2007).
[7] A. Ishida, S. Matsuura, M. Mizuno, Y. Sase, and H. Fujiyasu, J. Appl. Phys. **63**, 4572 (1988).
[8] B. B. Houston, R. F. Bis, and E. Gubner, Bull. Am. Phys. Soc. **6**, 436 (1961).
[9] H. R. Riedl, J. R. Dixon, and R. B. Schoolar, Phys. Rev. **162**, 692 (1967).
[10] J. R. Anderson, M. Gorska, Y. Oka, J. Y. Jen, I. Mogi, and Z. Golacki, Physica B **216**, 307 (1996).
[11] A. Y. Ueta, P. H. O. Rappl, H. Closs, P. Motisuke, E. Abramof, V. R. dos Anjos, V. A. Chitta, J. A. Coaquira, N. F. Oliveira, Jr., and G. Bauer, Braz. J. Phys. **34**, 672 (2004).
[12] B. Diaz, P. H. O. Rappl, and E. Abramof, J. Cryst. Growth **308**, 218 (2007).
[13] S. M. Sze, *Physics of Semiconductor Devices*, 2nd ed. (Wiley, New York, 1981), Chap. 1.
[14] A. Ishida, T. Yamada, D. Cao, Y. Inoue, M. Veis, and T. Kita, J. Appl. Phys. **106**, 023718 (2009).
[15] Y. W. Tsang and M. L. Cohen, Phys. Rev. B **3**, 1254 (1971).